Artificial neural network motor control for full-electric injection moulding machine

Veligorskyi, O., Chakirov, R., Khomenko, M. and Vagapov, Y.

This is a paper presented at the IEEE International Conference on Industrial Technology, Melbourne, Australia, 13-15 Feb. 2019.

Artificial Neural Network Motor Control for Full-Electric Injection Moulding Machine

Oleksandr Veligorskyi
Bonn-Rhein-Sieg University of Applied Sciences
Sankt Augustin, Germany
oleksandr.velihorskyi@h-brs.de

Roustiam Chakirov
Bonn-Rhein-Sieg University of Applied Sciences
Sankt Augustin, Germany
Roustiam.Chakirov@h-brs.de

Maksym Khomenko
Chernihiv National University of Technology
Chernihiv, Ukraine
mr.homax@gmail.com

Yuriy Vagapov
Glyndwr University
Wrexham, UK
y.vagapov@glyndwr.ac.uk

***Abstract*—This paper proposes a new artificial neural network-based position controller for a full-electric injection moulding machine. Such a controller improves the dynamic characteristics of the positioning for hot runners, pin valve and the injection motors for varying moulding parameters. Practical experimental data and Matlab's System Identification Toolbox have been used to identify the transfer functions of the motors. The structure of the artificial neural network, which used positioning error and speed of error, was obtained by numerical modelling in Matlab/Simulink. The artificial neural network was trained using back-propagation algorithms to provide control of the motor current thus ensuring the required position and velocity. The efficiency of the proposed ANN-based controller has been estimated and verified in Simulink using real velocity data and the position of the injection moulding machine and pin valve motors.**

Keywords—injection moulding, motor drive, permanent magnet motors, brushless motors, artificial neural networks, control

I. Introduction

Plastic injection moulding (PIM) is the most common manufacturing process used to produce high-quality three-dimensional plastic parts with high production speed, high quality and high tolerance. It is widely used in the automotive industry where plastic parts replace metal ones, for household appliances and cases for computer equipment, etc. The plastic injection moulding market is expanding year-on-year, and in accordance to market analysis will reach 496 billion US dollars by 2025 [1] with a Compound Annual Growth Rate of 6.0%. Over 60% of plastic parts are produced by injection moulding technology [2], due to its low cost for extremely fast production of complex shapes, using so called injection moulding machines (IMM). The main drivers in the expansion of injection moulding technology are the IMM set-up time, the process repeatability, reliability, energy efficiency and its associated environmental issues. Much research has been devoted to the improvement of these different aspects of injection moulding.

A typical IMM consists of three main units: the injection unit, the mould unit and the clamp unit (Fig. 1). The injection unit consists of a motor driven ram-screw, hopper and heating (heating bands) parts.

The moulding is a repeatable process that has four stages with different parameters. The first stage is *preparation*, when the melted material, by means of rotation of reciprocating screw, moves to the front part of IMM and is placed at the front of the nozzle in the barrel. The second stage is *filling*, when the reciprocating screw moves forward, the non-return valve is closed by pressure inside the nozzle part, and the melted material then fills the mould cavity with controllable velocity. During this stage the screw moves linearly forward, providing the necessary level of pressure in the cavity, and the stage ends when mould cavity becomes full of plastic. After this, the *holding pressure* stage (or *post-filling* stage) starts, where a constant pressure is maintained, to provide additional material to the cavity in order to compensate for the volumetric shrinkage of material due to cooling. After the part inside the mould has adequately cooled, the final stage starts. This involves the mould opening to eject the moulded part and the reciprocating screw moving backward to the initial position, so that the process may be repeated.

With regard to the PIM process, the improvement of energy efficiency, moulding quality and repeatability of IMMs is possible by employing several techniques.

A. Quality of Injection Moulding

Although parameters such as the cavity pressure and plastic flowrate influence moulding quality, they are hardly measured [3]. However, the injection screw speed which affects the plastic flowrate, the pressure at the injection nozzle and the cavity pressure, is the reason why the speed of injection of the reciprocating screw (injection velocity) along with the injection nozzle pressure is used as control

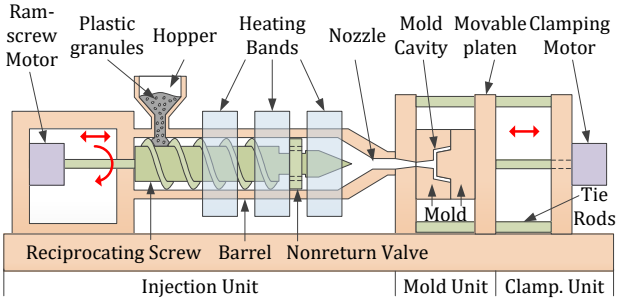

Fig. 1. Simplified injection moulding machine.

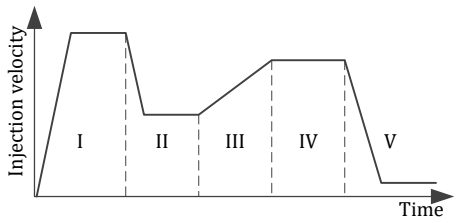

Fig. 2. Injection velocity profile during the filling process [4].

parameters in closed-loop IMMs [2], [3]. The injection velocity profile shown in Fig. 2 [4] has several zones, where the velocity is changed from a maximum level (zone I where the runner is filled by plastic) to provide minimum injection time and avoid heat losses in material, to a minimum level (zone V, end of mould filling) to provide elimination of flashing and over-packing of material. In zone II (melted plastic passes through the gate area) the velocity should be reduced to avoid jetting. Zones III and IV correspond to the filling of the mould cavity. Such velocity profiles eliminate many possible moulding problems, such as weld lines, jetting, short-spot, etc. The amplitude of the pressure in different zones, as well as its duration depends on the cavity and the material properties [4]. A high quality of moulding is possible with the precise control of the injection velocity, providing there exists a good correspondence of the real position and velocity of the screw with the injection velocity profile (Fig. 2), without overshoots and with a minimum static and dynamic error.

As it has been shown in [5], the pressure can be modelled by a first-order plus time-delay model superimposed on a constantly increasing (ramp) pressure component for the filling mode. Under this mode, the cavity pressure increased when melted polymer is filling the cavity [4]. The other issue is, as it was mentioned before, injection moulding has four zones with different properties, and mould parameters are different for each zone. This is why (nonlinearity and time-varying injection dynamics) the control of the injection velocity and pressure is difficult using classical controllers such as PID. Similarly, changing the mould may lead to different system parameters, and a previously tuned controller will not provide a good quality of moulding. So, artificial intelligence-based controllers (such as Fuzzy, ANN or ANFIS) can provide the high quality regulation for different moulding parameters. Already published papers analysed modern AI controllers for injection moulding based on fuzzy logic control [2], [4], [6], [21]. Meanwhile, many other modern control techniques have been analysed for plastic moulding, such as adaptive sliding mode control [1], [22] model-predictive control (MPC) [3].

B. Electric Drive in IMM

All of the above mentioned papers are devoted to the control of IMM, controlled by the pneumatic valve for a linear moving and rotating screw, which provides the necessary pressure of melted plastic before and during the injection. It should be noted that an appropriate operation of electric drive can significantly increase energy efficiency and moulding quality. There are two types of movements in IMM: linear and rotational. Such movements as the clamp movement/injection (linear) and metering/plasticising (rotation), about the "3 main axes" of the IMM, require the highest power [7]. Additional axes consist of drive for nozzle contact, ejection, pin for nozzle valve gate (linear), unscrewing device (rotation). Some IMMs have a hydraulic transmission power system, in which oil pumps are driven by AC electric motors. In such machines, the motor provides revolving speed and power, and the oil pump transmits mechanical energy of rotation to the pressure energy for movement of the movable platen, reciprocating screw, etc. This class of IMMs is called "*hydraulic IMMs*".

"*Hybrid IMMs*" have at least one of 3 main axes driven by an electric servo-motor, a brushless direct current motor (BLDC) or a permanent magnet synchronous motor (PMSM), without hydraulic transmission system. Taking into account that the plastic metering requires a greater share of the energy compared to other movements, servo-drive metering IM machines are the most popular among hybrid IMMs. "*Servo-hydraulic IMMs*" have hydraulic transmission systems for all axes, but instead of using unregulated AC drive all of the oil pumps are driven by servo-motors, and this significantly improves energy efficiency [7].

"*Full-electric IMMs*" have no hydraulic transmission for any of the 3 main axes, and operate by servo-motors [8], providing all movements, including movement and rotation of ram, nozzles in valves for hot runner systems [9], unscrewing devices, etc. "Full-electric" PIM machines have many advantages, such as: better moulding repeatability and moulding precision due to smooth injection, lower power energy consumption (e.g. 80% less for clamping unit [10] and less than half the total power consumption); no oil or other liquids that could lead to pollution, which is especially important for clean rooms (moulding of medical parts, etc.). It should be noted, that in accordance to Euromap 60 standard, additional axes in "full-electric" machines can be hydraulic or servo-driven too. Nevertheless, the use of electric drives for valve pin movement in hot runner PIM systems significantly improves quality, eliminating weld-lines and other drawbacks of uncontrollable injection through the runner nozzle. A typical position profile is depicted in Fig. 3. The duration and pin speed depends on part size, material, etc.

Several papers have analysed the use of electric drives in IMMs. In [11] the motor drive system based on a model predictive control for an IMM has been proposed, but the IMM has been analysed separately, one part of the work was

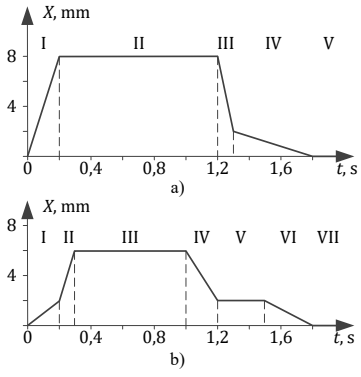

Fig. 3. Valve pin position profile in eGate® hot runner systems [9].

devoted to the transfer function (TF) of the IMM, and another one – for the MPC of the Permanent Magnet Synchronous Motor (PMSM). However, it has not been shown how the velocity of the PMSM will influence the pressure in the mould or nozzle. Authors of [12]-[14] proposed a two-loop control system for full-electric IMM, including speed (for AC servo motor) and force (for nozzle pressure) loops equipped with PI-controllers. Taking into account practical problems with pressure sensors (e.g. price, different position of such sensor in conventional servo systems), the authors proposed sensorless force control based on a reaction force observer [12] high-order reaction force observer [13] and Friction-Free Observer [14], which suppressed the effect of the static friction and eliminated steady-state pressure error during the pressure holding process, caused by torque transmission losses in the mechanical structures of drive (gears, ball screw, etc.).

This paper proposes a new position controller based on ANN for electric drives in full-electric IMMs. Electrical and mechanical models of 3-phase motors have been analysed in the section II of this paper. The Motor's transfer functions have been experimentally identified in the section III. Section IV includes the results of the training and employment of ANN-based position controller for IMM's pin valve and injection motors. The efficiency of the proposed ANN controller was validated by numerical modelling in Matlab/ Simulink.

II. Three-Phase Motor Models

The first step to control any process, including motors, is obtaining the information about the control object. Different type of representations for BLDC and PMSM motors can be used, including electrical and mechanical models, state-space or vector models [15], [16]. Let's consider the electrical part of 3-phase motors, taking into account that all motor's phase and their parameters are identical.

A. Electrical model of three-phase motor

A simplified electrical and mechanical part of the three-phase motor's model is shown in Fig. 4 Considering three windings of the motor, the next expression is used to describe the processes:

$$\bar{V}_S = R_S \bar{i}_S + \frac{d\bar{\psi}_S}{dt} \tag{1}$$

where $\bar{V}_S = |V_a \; V_b \; V_c|^t$ and $\bar{i}_S = |i_a \; i_b \; i_c|^t$ are vectors of stator voltage and current, $R_S = R_{Sa} = R_{Sb} = R_{Sc}$ is winding resistance, $\bar{\psi}_S = |\psi_a \; \psi_b \; \psi_c|^t$ are vector of stator flux linkage.

$$\bar{\psi}_S = L_S \bar{i}_S + \psi_m e^{j\theta_r} \tag{2}$$

where $L_S = L_{Sa} = L_{Sb} = L_{Sc}$ is self-inductance of stator, ψ_m is magnitude of stator flux linkage, θ_r is position of magnetic axis of rotor compare to stator windings.

$$\bar{V}_S = R_S \bar{i} + L_S \frac{d\bar{i}}{dt} + j\psi_m \omega_r e^{j\theta_r} = R_S \bar{i} + L_S \frac{d\bar{i}_S}{dt} + \bar{e}(t) \tag{3}$$

where $\bar{e}(t)$ is back electromotive force (EMF) of the motor, $\omega_r = d\theta_r/dt$ is electric angular frequency of motor.

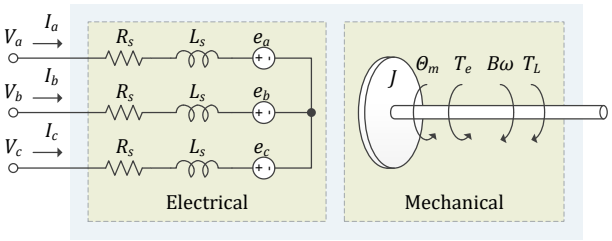

Fig. 4. Electrical and mechanical model of 3-phase motor.

Type of electric motor defines the shape of back-EMF: for PMSM it is sinusoidal, whereas for BLDC it is trapezoidal. Taking into account that the back-EMF in three-phase motor is shifted by 120°, they can be expressed as follows:

$$e_a = k\omega_m f(\theta_r), e_b = k\omega_m f\left(\theta_r - \frac{2\pi}{3}\right), \quad e_c = k\omega_m f\left(\theta_r + \frac{2\pi}{3}\right) \tag{4}$$

where k is back-EMF constant, ω_m is mechanical rotor velocity, $f(\theta_r)$ is function of back-EMF.

It should be noted, that PMSM and BLDC motors has several permanent magnets, so, $\omega_r = \omega_m p/2$, $\theta_r = \theta_m p/2$, where θ_m is mechanical rotor angle, p is number of pole pairs in motor (p = 4, 6, 8, 10 etc.).

By means of Laplace transformation of expression (3) we can obtain the electric transfer function of motor:

$$W_e(s) = \frac{\bar{i}_S(s)}{\bar{V}_S(s) - \bar{e}(s)} = \frac{1}{L_S s + R_S} \tag{5}$$

where s is a Laplace operator variable.

B. Mechanical Model of Motor

Simplified mechanical part of the three-phase motor is shown in Fig. 4. Motor electromagnetic torque T_e, produced by magnetic forces caused by phase currents, can be calculated as follows:

$$T_m = \frac{i_a e_a + i_b e_b + i_c e_c}{\omega_r} = K_t \left[i_a f(\theta_r) + i_b f\left(\theta_r - \frac{2\pi}{3}\right) + i_c f\left(\theta_r + \frac{2\pi}{3}\right) \right] \tag{6}$$

where K_t is torque coefficient. Electromagnetic torque is equalized by inertia of rotating rotor, load torque and friction:

$$T_m = J\frac{d\omega_m}{dt} + B\omega_m + T_L \tag{7}$$

where J is inertia of rotor, B is friction coefficient, T_L is load torque. By means of Laplace transformation of expression (7) we can obtain the mechanical transfer function of motor:

$$W_m(s) = \frac{\omega_m(s)}{T_m(s) - T_L(s)} = \frac{1}{Js + B} \tag{8}$$

Such first-order mechanical transfer function is typical for the motor with rigid connections of motor and gear, and widely used in many cases. Similarly, electric drives in IMMs often have a ball screw in linear actuator parts (e.g. gears for

TABLE I. MOTOR'S TECHNICAL PARAMETERS

Parameter	*Nanotec*	*Exlar*
Voltage, rated, V	48	400
Current, rated, A	6.9	1.2
Winding resistance R_s, Ohm	0.28	36.3
Winding inductance L_s, mH	1.3	96.8
Electromagnetic torque T_m, Nm	0.9	1.84
Torque constant K_t, Nm/A	0.13	1.75
Rotor inertia J, g·cm^2	544	30

injection and pin nozzle of valve gate). The presence of a ball screw unit, as it known, leads to resonance in the gear caused by the torsional vibration frequencies in the shafts. In such cases, the transfer function of mechanical part (motor and linear actuator) has a third-order and could be presented as follows [12]:

$$W_m(s) = \frac{b_1 s^2 + a_3 b_1 s + a_4 b_1}{s^3 + (a_1 + a_3)s^2 + (a_1 a_3 + a_2 a_5 + a_4)s + a_1 a_4 + a_2 a_3 a_3} \quad (9)$$

where coefficients b_i and a_j depend on motor, gear and load parameters. Taking into account difficulties in analytical identification of such motor parameters, as well as fact that some parameters depends on load and are not described in motor documentation, experimental identification of motor's model parameters is carried out in the paper.

III. IDENTIFICATION OF MOTOR TRANSFER FUNCTIONS

Two types of three-phase motors are considered in the paper, BLDC Nanotec DB80S048030-ENM05J, and PMSM Exlar GSM30-1201IFFRA3-158-30; both motors are equipped with an incremental encoder. Technical parameters of motors are shown in Table 1.

To obtain parameters of model, series of positioning experiments has been carried out. Motor drives Elmo CEL-15RMS/60 and Infranor XtrapulsPac Pac-ak-400/20-ST was used to control 8-poles, 3000 rpm Nanotec and Exlar motors, respectively. Parameters of current, speed and position controllers for motor drives were obtained by auto-tuning

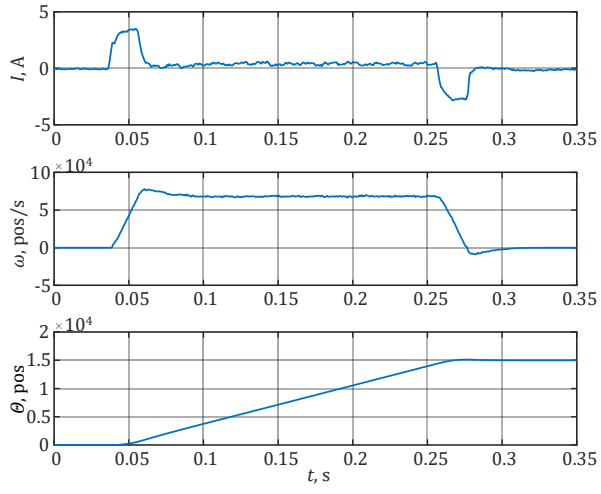

a)

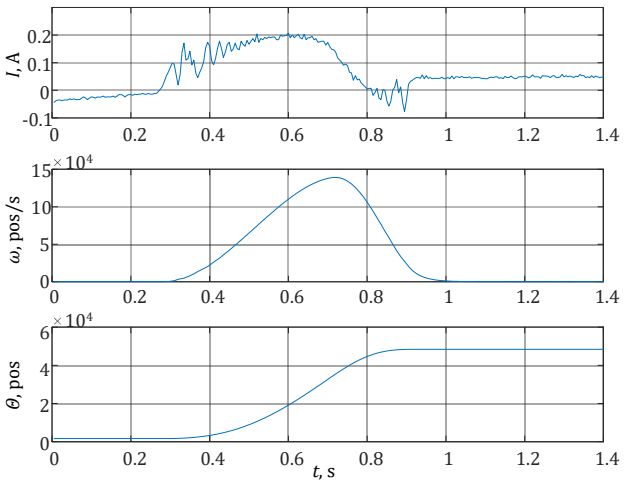

b)

Fig. 5. Experimental positioning of BLDC (a) and PMSM (b) motors.

TABLE II. PARAMETERS OF MOTOR TRANSFER FUNCTIONS

Motor	b_2	b_1	b_0	a_3	a_2	a_1	a_0
Nanotec	8.48×10^9	3.46×10^{13}	2.79×10^{13}	1	2.58×10^7	2.39×10^8	6.42×10^4
Exlar	0	6.32×10^6	2.69×10^8	1	44.73	309.3	241

procedure by means of Elmo Composer and Gem Drive Studio software. That software was also used to acquire current, speed and position data sets, represented in Fig. 5. It should be noted, that speed and position is measured by using encoder pulses instead of rotation or linear displacement.

Then, all signal processing was performed in Matlab software. The first step is the filtering because these signals are noisy as it is clearly seen from current graphs (Fig. 5). Taking into account large frequency span of current signal, Savitzky-Golay smoothing filter was used (*sgolay* function). The next task is identification by means of *System Identification Toolbox* in Matlab. Current and speed were used as input and output working data sets for identification. To validate the quality of identification other time series for positioning was used.

Results of motor parameters identification are presented in Table II. Example of comparison for Nanotec BLDC motor shown in Fig. 6 proves a good correspondence of actual experimental data and response for identified transfer functions.

As mentioned earlier in this paper, ANN-based controllers can provide high quality regulation of IMMs for different moulding parameters. So a controller based on ANN was designed for the motor positioning in this paper. The position control system for one axis of an IMM is shown in Fig. 7.

IV. ARTIFICIAL NEURAL NETWORK CONTROLLER FOR IMM

An artificial neuron is a first approximation that simulates the biological neuron, while neural network is a set of neurons connected to each other. The topology of the ANNs can be divided into three main groups: full-mesh, weakly connected networks, multilayer network. Nowadays it is

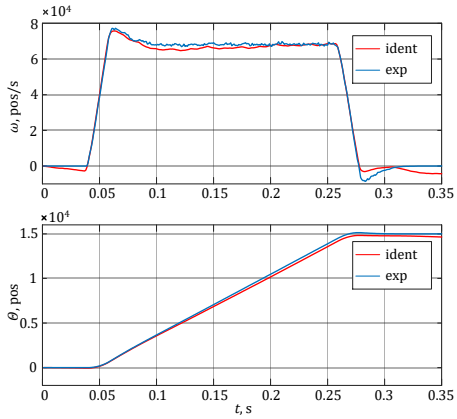

Fig. 6. Comparison of motor positioning: experimental and identified transfer function.

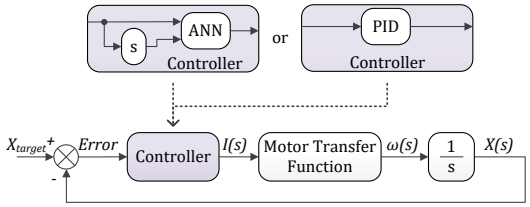

Fig. 7. Position control system.

widely recognised that multilayer network is one of the best topology for automated control systems [17]-[19].

The radial basis function networks (RBF) and recurrent networks are also used in control system applications. However, the RBF networks usually have a larger quantity of neurons compared to a feed forward network (FFN) for the same application [17]. The recurrent network itself is a dynamic system with highly-nonlinear parameters [17], [20] so implementation of such a network in the control loops leads to computational complexity growth.

So, an offline-trained multilayer FFN was chosen for the position controller implementation because of its strong approximation ability and relatively small computational complexity. Position error and speed of position error changing was used as inputs of the ANN because they give a good representation of system dynamics. The network itself consists of two hidden layers – 2 neurons in the 1-st hidden layer and 2 neurons in the 2-nd hidden layer. The activation function of all neurons in hidden layers is a hyperbolic tangent function because such types increase the learning efficiency [17]. The output layer consists of one neuron with a linear activation function. The output of this layer should be in the gap from −6.9 to 6.9 A, which is limited by the motor.

The ANN should be trained offline before being used in the position control system. The training data set should be regularly distributed upon the entire range of possible input values (position error and speed of changing position error) to ensure the best approximation capability of the network. The ANN was trained by means of data sets, representing positioning of the motor for injection velocity profile (Fig. 2, for PMSM Exlar motor), and valve pin position profile (Fig. 3, for BLDC Nanotec motor). The amplitude of the training set signals was increased in the range from 0 to maximum possible displacement of valve pin or reciprocating screw. A

TABLE III. RMS OF PIN NOZZLE POSITIONING

RMS	Normal			Slow		
	2 mm	*6 mm*	*10 mm*	*2 mm*	*6 mm*	*10 mm*
PID, mm	0.759	0.246	0.022	2.268	0.729	0.064
ANN, mm	0.702	0.229	0.024	1.876	0.654	0.081
Diff., %	8.12	7.42	−8.33	20.9	11.47	−20.99

Levenberg-Marquardt algorithm, one of the most efficient back propagation algorithms based on the conjugate gradient method, was used to training ANN. As a result, the weight coefficient and number of neurons in each layer was obtained.

The results of ANN controller implementation in the pin valve positioning system are shown in Fig. 8 for nominal and a variation of the motor's parameters (slowed TF represent pin valve with melted plastic, increasing load inertia of the system). Root mean square error for different position profiles are collected in Table III, calculated as follows:

$$\mathrm{RMS} = \sqrt{\frac{\sum_{i}^{n} Error_i^2}{n}} \qquad (10)$$

$$\mathrm{Diff} = \frac{\mathrm{RMS_{PID}} - \mathrm{RMS_{ANN}}}{\mathrm{RMS_{ANN}}} \times 100\%$$

As it is clearly seen the ANN controller provides more precise control for higher displacement of nozzle pin whereas PID controller works better for small ones where nonlinear behaviour of system does not appear and output controller current does not reach limit of 6.9 A. In the same time, overshoot for ANN is higher compared to PID.

V. CONCLUSION

This paper presents ANN-based controller for positioning of injection screw and pin nozzle in full-electric injection plastic moulding machines. The transfer functions of different 3-phase motors were analysed including the electrical and mechanical parts. A 3rd order transfer function was used taking into account that the analysed motors operate as linear actuators containing a ball screw. The transfer function coefficients of the motor were identified in the Matlab software environment using System Identification Toolbox and experimental positioning data for two motors. An ANN controller with two input parameters (position error and speed of position error) was trained by means of Matlab Neural Network Toolbox. Simulation of the designed closed-loop positioning system with PID- and ANN-controllers shows that the ANN-based controller operates in a wide range of motor load parameters, inherent in the operation of IMM. The proposed controller is recommended for full-electric IMMs instead of classical controllers for closed-loop motor drives system.

ACKNOWLEDGMENT

The current work was supported by German Central Innovation Program for SMEs (Zentrales Innovationsprogramm Mittelstand) from Federal Ministry for Economic Affairs and Energy (Bundesministeriums für Wirtschaft und Energie), project № ZF4190302DB6.

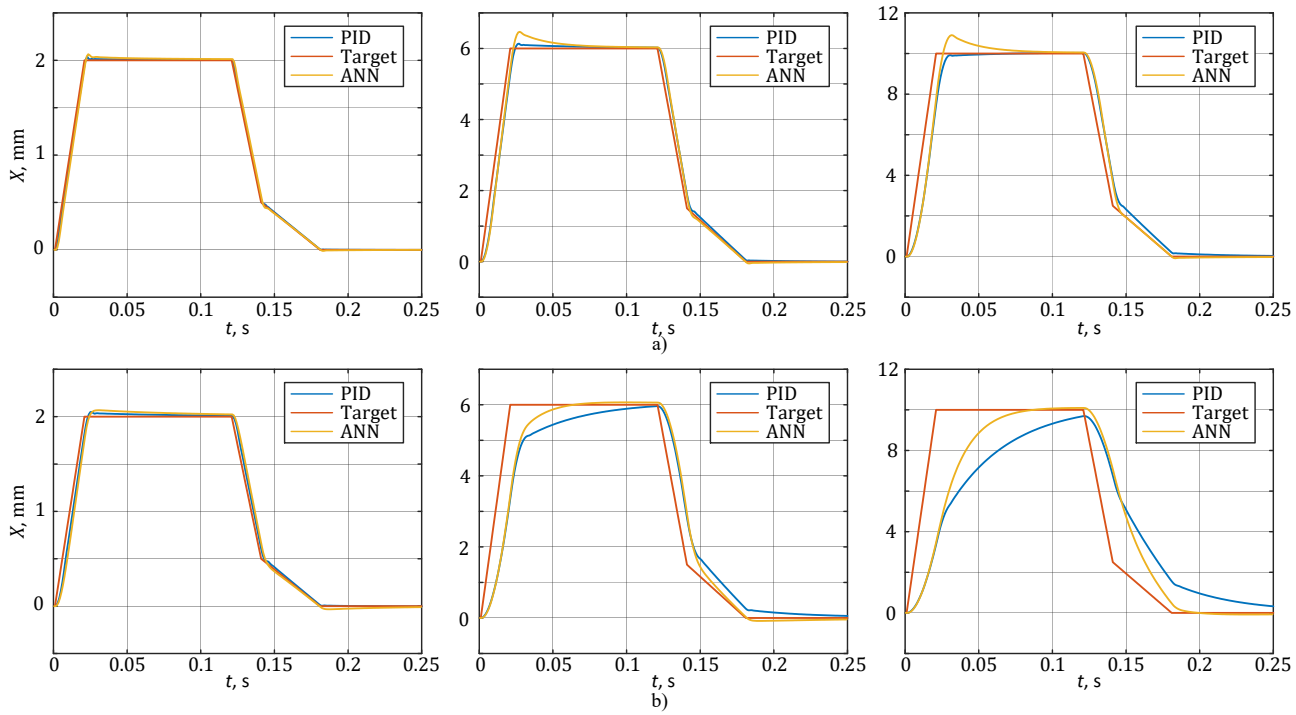

Fig. 8. Comparison of PID and ANN controller for valve pin position at various profiles, nominal (a) and slowed (b) transfer functions of Nanotek motor.

REFERENCES

[1] Grand View Research (2018, Feb). Injection Molded Plastics Market Size Worth $496.22 Billion By 2025. [Online]. Available at: https://www.grandviewresearch.com/press-release/global-injection-molded-plastics-market

[2] S.-J. Huang, and T.-H. Lee, "Fuzzy logic controller for a retrofitted closed-loop injection moulding machine," *Proc. of IMechE, Part I: J. Syst. Control Eng.*, vol. 214, no. 1, pp. 9–22, Feb. 2000.

[3] R. Dubay, B. Pramujati, J. Han, and F. Strohmaier, "An investigation on the application of predictive control for controlling screw position and velocity on an injection molding machine," *Polymer Eng. Sci.*, vol. 47, no. 4, pp. 390–399, April 2007.

[4] H.P. Tsoi, and F. Gao, "Control of injection velocity using a fuzzy logic rule-based controller for thermoplastics injection Molding," *Polymer Eng. Sci.*, vol. 39, no. 1, pp. 3–17, Jan. 1999.

[5] M.R. Kamal, W.I. Patterson, N. Conley, D. Abu Fara, and G. Lohfink, "Dynamics and control of pressure in the injection molding of thermoplastics," *Polymer Eng. Sci.*, vol. 27, no. 18, pp. 1403–1410, Oct. 1987.

[6] Feriyonika-Feriyonika, and G. Dewantoro, "Fuzzy sliding mode control of injection velocity in injection molding during filling phase," in *Proc. 2nd Int. Conf. Instrumentation Control Automation*, 15-17 Nov. 2011, Bandung, Indonesia, pp.134–139.

[7] M. Klaus, "15 things to know about servo-driven injection machines," *Plastics Technology*, vol. 63, no. 3, pp. 46–51, March 2017.

[8] Fanuc (2018, Oct. 31). High-performance, high-reliability and high-productivity electric injection molding machine, with Fanuc standard CNC installed. Fanuc Roboshort α-SiA series. [Online]. Available at: https://www.fanuc.co.jp/en/product/roboshot/index.html

[9] Synventive Molding Solution (2018, Nov. 23). eGate® Electric Valve Gate. [Online]. Available at: http://www.synventive.com/egate.aspx

[10] Xcentric Mold and Engineering (2018, Nov. 23). About Injection Molding [Online]. Available at: https://www.xcentricmold.com/about-injection-molding

[11] G.Hu, A. Xia, Z. Li, and Z. Mei, "Research on injection molding machine drive system based on model predictive control," in *Proc. 2nd Int. Conf. Robotics Automation Eng.*, 29-31 Dec. 2017, Shanghai, China, pp. 161–167.

[12] Y. Ohba, M. Sazawa, K. Ohishi, T. Asai, K. Majima, Y. Yoshizawa, and K. Kageyama, "Sensorless force control for injection molding machine using reaction torque observer considering torsion phenomenon," *IEEE Trans. Ind. Electron.*, vol. 56, no. 8, pp. 2955–2960, Aug. 2009.

[13] R. Furusawa, T. Asai, K. Ohishi, K. Majima, K. Kageyama, M. Takatsu, and S. Urushihara, "High-performance sensorless injection force control based on nonlinear friction phenomenon," in *Proc. 36th Ann. Conf. of IEEE Ind. Electron. Soc. IECON-2010*, 7-10 Nov. 2010, Glendale, AZ, USA, pp.858–863.

[14] K. Iwazaki, K. Ohishi, Y. Yokokura, K. Kageyama, M. Takatsu, and S. Urushihara, "Robust sensorless pressure control of electric injection molding machine using friction-free force observer," in *Proc. 13th IEEE Int. Workshop Advanced Motion Control*, 14-16 March 2014, Yokohama, Japan, pp. 43–48.

[15] J. Kabzinski, Ed., *Advanced Control of Electrical Drives and Power Electronic Converters*. Zurich, Switzerland: Springer, 2017.

[16] S. Preitl, A.-I. Stinean, R.-E. Precup, Z. Preitl, E.M. Petriu, C.-A. Dragos, and M.-B. Radac, "Controller design methods for driving systems based on extensions of symmetrical optimum method with DC and BLDC motor applications," *IFAC Proc. Volumes*, vol. 45, no. 3, pp. 264–269, March 2012.

[17] S. Haykin, *Neural Networks: A Comprehensive Foundation*, 2nd ed., New Delhi, India: Prentice-Hall, 2008

[18] F. Rios-Gutierrez, and Y. Makableh, "Efficient position control of DC servomotor using backpropagation neural network", in *Proc. 7th Int. Conf. Natural Computation*, 26-28 July 2011, Shanghai, China, vol. 2, pp. 653–657.

[19] M. Cirstea, A. Dinu, J.G. Khor, and M. McCormick, *Neural and Fuzzy Logic Control of Drives and Power Systems*. Oxford: Newnes, 2002.

[20] D. Prokhorov, "Training recurrent neurocontrollers for real-time applications," *IEEE Trans. Neural Netw.*, vol. 18, no. 4, pp. 1003–1015, July 2007.

[21] J.L. Lian "Self-organizing fuzzy controller for injection molding machines," *J. Process Control*, vol. 20, no. 5, pp. 585–595, June 2010.

[22] K.K. Tan, S.N. Huang, and X. Jiang "Adaptive control of ram velocity for the injection moulding machine," *IEEE Trans. Control Syst. Technol.*, vol. 9, no. 4, pp. 663–671, July 2001.